

METHODS & TECHNIQUES

Development of a vortex generator to perturb fish locomotion

Deeksha Seth^{1,*}, Brooke E. Flammang², George V. Lauder³ and James L. Tangorra¹

ABSTRACT

Knowledge about the stiffness of fish fins, and whether stiffness is modulated during swimming, is important for understanding the mechanics of a fin's force production. However, the mechanical properties of fins have not been studied during natural swimming, in part because of a lack of instrumentation. To remedy this, a vortex generator was developed that produces traveling vortices of adjustable strength which can be used to perturb the fins of swimming fish. Experiments were conducted to understand how the generator's settings affected the resulting vortex rings. A variety of vortices (14–32 mm diameter traveling at 371–2155 mm s⁻¹) were produced that elicited adequate responses from the fish fins to help us to understand the fin's mechanical properties at various swimming speeds (0–350 mm s⁻¹).

KEY WORDS: Fish swimming, Vortex ring, Perturbation, Stiffness, Mechanical properties, Bluegill sunfish

INTRODUCTION

Many studies have concluded that fish modulate the stiffness of their fins during swimming (Bainbridge, 1958; Hunter and Zweifel, 1971; McHenry, et al., 1995; Long and Nipper, 1996; Long, et al., 2006; Flammang and Lauder, 2008; Curet, et al., 2011; Flammang, et al., 2013) but this has not been tested directly on swimming fish. This is due, in large part, to a lack of experimental devices that can interrogate fins without impeding the fish's natural swimming motion. One method for understanding the mechanical properties of fish fins *in vivo* is to perturb the fins while they are used in locomotion, and observe the response to perturbations of various strengths.

Based on perturbation studies conducted to evaluate human physiological responses (Marmarelis and Marmarelis, 1977; Kearney and Hunter, 1982; Bennett et al., 1992; Tangorra, et al., 2003), it was hypothesized that a fin's stiffness could be evaluated by measuring its response to an external fluidic perturbation. The perturbation would have to be aimed and modulated in strength for different fins, develop and travel in free-stream flows of different speeds, be applied as the fish swims freely, interact with the fin over a short period relative to the fin beat duration, and cause measurable deflection in the fin without stopping the fish's natural swimming. The relative stiffness changes in the fin can be quantified by comparing the deflections in the fin caused by vortex rings of

known strengths. The strengths of the vortex rings can be estimated using the vortex size, speed and circulation (McErlean, 2011). To meet these needs, we have developed a device that generates vortices suitable for conducting perturbation studies with sunfish swimming at speeds between 0 and 350 mm s⁻¹.

Previously, vortex generators have been developed as underwater thrusters (Gharib, et al., 1998; Krueger and Gharib, 2003; Dabiri and Gharib, 2005; Mohseni, 2006), but the designs are not, simultaneously, sufficiently small and adjustable to produce vortices with the desired range of size and strength. Studies of these vortex generators did not discuss the vortices as individual rings traveling over distances at which the fish was expected to swim, and most previous aquatic generators developed as thrusters produced a fluid jet and not a discrete perturbation pulse. To be applied to freely swimming fish, a new vortex generator design needed to be developed and individual vortex rings needed to be studied as stimuli, in both static and flowing water.

MATERIALS AND METHODS

Design requirements

To be useful for biological studies, a vortex ring should form quickly, maintain its shape, size and speed while traveling to the swimming fish, have a minimum trailing jet, interact with the fin for a short duration, and be of appropriate strength to cause a measurable deformation of the fin without stopping the fish's natural swimming. Perturbation studies are conducted on different fish over a range of swimming speeds so it is crucial to be able to adjust attributes of the vortex. Based on preliminary experiments with fish, the diameter of the ring must range from 5 to 30 mm, speeds more than 400 mm s⁻¹ should be achieved, the ring must separate from the trailing jet within 100 mm of its initial travel so that the impact duration is short, the ring must maintain its shape and velocity for at least 150 mm so that it can impact the fish throughout the testing tank, and the ring should be discrete and well-formed when impacting the fin.

Physically, the vortex generator needs to be compact in size and capable of being inserted into an aquarium or flow tank and aimed at fish fins from different heights and angles. It also needs to have settings that can be adjusted whilst the generator is in the tank. Based on the size of the tank for these experiments and the expected positions of the fish, the device had to be no larger than 70×40×100 mm (length×width×height), and aim at angles between -60 and +60 deg.


Mechanical design

The vortex generator consists of an underwater cavity from which the vortex is ejected, a reservoir (X2 Industries, St Croix Falls, WI, USA) of pressurized water that provides the motive force, and a computer-controlled electronic solenoid (STC Valve, Palo Alto, CA, USA) that controls the flow of water from the reservoir. The underwater cavity has an open end that is covered by an orifice plate and contains a ball that travels within the cavity. Vortices are created by accelerating the ball through the cavity and ejecting a slug of

¹Drexel University, Department of Mechanical Engineering and Mechanics, 3141 Chestnut Street, Randall 115, MEM Department, Philadelphia, PA 19104, USA.

²New Jersey Institute of Technology, Department of Biological Sciences, University Heights, Newark, NJ 07102, USA. ³Harvard University, Department of Organismic and Evolutionary Biology, Museum of Comparative Zoology Laboratory, 26 Oxford Street, Cambridge, MA 02138, USA.

*Author for correspondence (deeksha.seth@drexel.edu)

 D.S., 0000-0003-4297-0286

water through the orifice (Figs 1 and 2B). The ball provides a clean separation of the vortex from the orifice as it seals the cavity as the vortex departs, and minimizes the trailing jet.

The underwater cavity is machined out of clear polycarbonate so that the ball is visible when adjusting its initial position. Two cylinders with different diameters were used: cavity 1, 13 mm inner diameter (i.d.), and cavity 2, 20 mm i.d. The orifice plates were machined out of 0.5 mm aluminium and are held onto the ejection end of the cavity with a clip that allows orifice plates with different diameters to be used. The cavity is supported on a rod, which allows the cavity to be positioned at different angles.

Functionality

Vortex characteristics are tuned by adjusting the pressure in the reservoir, the duration for which the solenoid valve is open, the ratio of the orifice to the cavity diameter, and the ball's initial position. Reservoir pressure and the time the valve is open are controlled using a regulator (Norgren B07-202-A1KA) and microcontroller (Arduino Duemilanove, ATmega328), respectively. The ratio of orifice and cavity diameters is adjusted by selecting the appropriate orifice plate (Fig. 1B). The amount of water that will be released from the cavity is set by manually positioning the ball at the beginning of each experiment. The water pressure (P), duration the valve is open (t_{valve}), ratio of orifice and cavity diameters (d/D), and distance traveled by the ball (stroke length, L_{stroke}) are collectively referred to as the 'perturber settings'. Once the perturber settings are configured, the test is initiated by opening the solenoid via the microcontroller.

Experiments and data collection

Experiments

Experiments were conducted to understand how the perturber settings affected the formation, size and speed of the vortex. The effect of flow on the vortex was also considered. Each cavity (13 and 20 mm) was tested at reservoir pressures of 7–217 kPa, at intervals of 14 and 24 kPa. These increments were selected because they

led to measurable changes in the vortex outcomes during the prototyping phase. At each pressure, two t_{valve} values (20 and 40 ms) and two d/D values (0.9 and 0.6) were tested. The 13 mm cavity was tested using two L_{stroke} values (25 and 45 mm) and the 20 mm cavity was tested with one (35 mm). All fish were handled ethically according to Harvard University Institutional Animal Care and Use Committee guidelines (IACUC protocol 20-03).

Data collection

The vortices were imaged using high-speed cameras (Exilim Pro EX-F1, Casio, USA, at 300 frames s^{-1} or PCI 1024, Photron Inc., San Diego, CA, USA, at 1000 frames s^{-1}). The attributes of vortices were determined from images using MATLAB (<http://www.mathworks.com/matlabcentral/fileexchange/24279-image-measurement-utility>).

Vortex analysis

Vortices were analyzed during formation, propagation and impact. During formation, the pressurized water pushed the ball, which accelerated a fluid slug out of the cavity. The vortex separated from an axial jet ('starting jet', Fig. 2D) at a distance referred to as the 'separation distance'. During separation, the length of the residual jet is called the 'trailing jet length during separation' (Fig. 2D) (Gharib, et al., 1998). During propagation, the vortex translated, and any trailing jet either dissipated or traveled with the vortex. Vortex size and translation speed were measured. During impact, the vortex interacted with a fin or foil placed about 100 mm away from the perturber. The length of the residual jet was measured again and is called the 'trailing jet length during impact'. In experiments with no fin or foil, the trailing jet's length was measured when the vortex had traveled 100 mm. These parameters (size, speed, separation distance and lengths of trailing jets) will be referred to as 'vortex characteristics'.

RESULTS AND DISCUSSION

The device successfully produced vortices that met the criteria for perturbing the fins of freely swimming fish (Fig. 2C,E; Movie 1). The

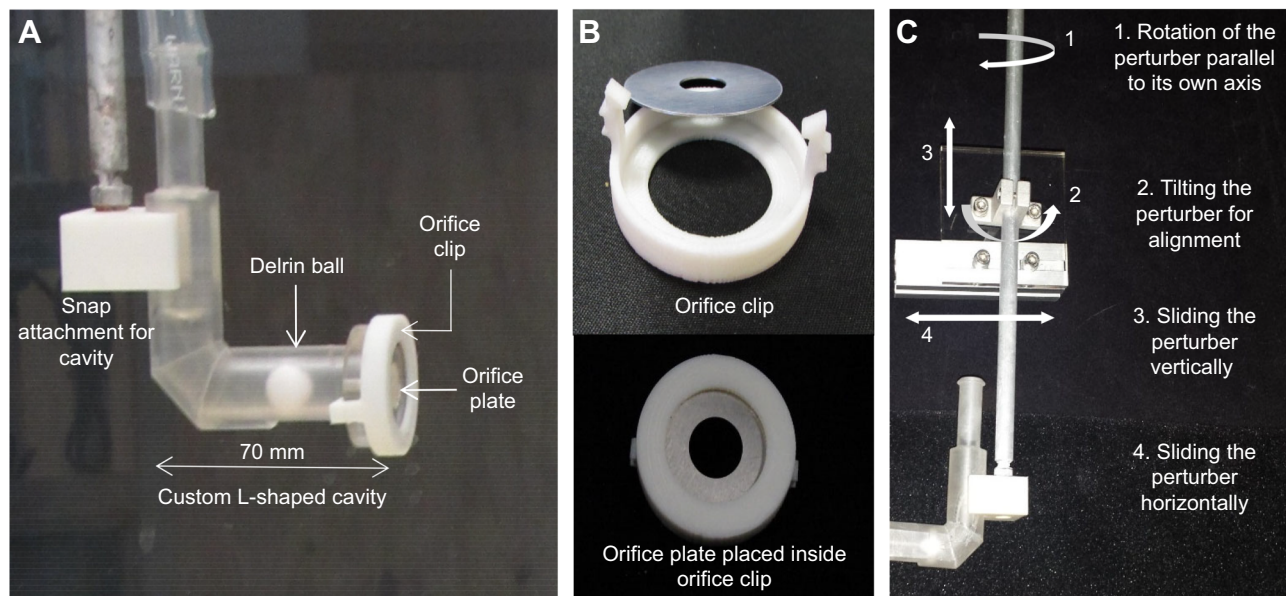


Fig. 1. Sub-systems of the vortex generator. (A) L-shaped cavity assembly, placed underwater, consisting of the ball acting as a piston and the orifice plate secured with the orifice clip. (B) Images of clips used to secure orifice plates at the ejection point on the cavity and to allow easy swapping of orifice plates to change the orifice diameter when needed. (C) Assembly that holds the cavity in place underwater and allows for different orientations. Note the cavity set up was moved closer to the assembly for the picture. In the experiments, the orientation control is farther from the cavity and out of the water for easy access.

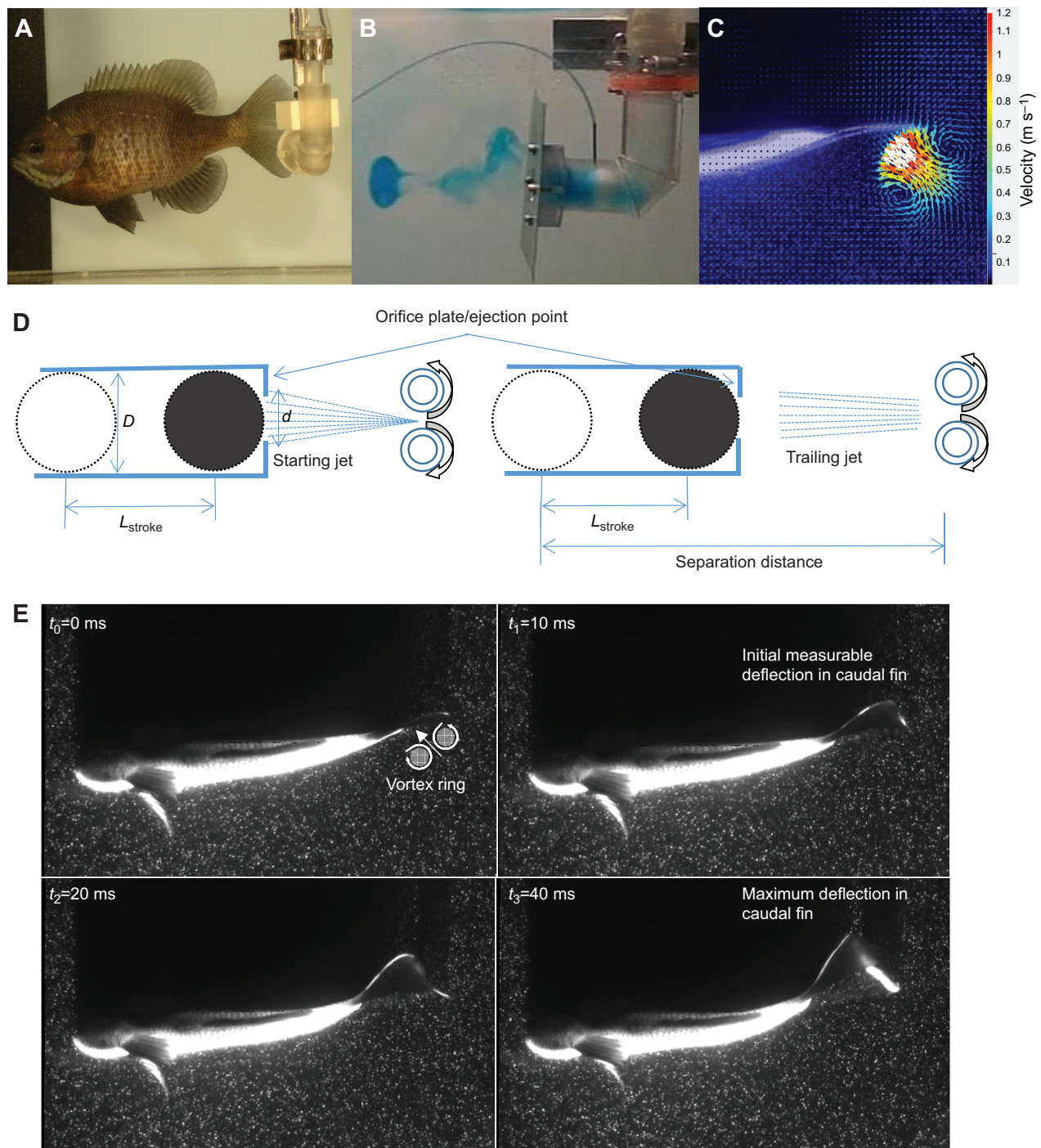


Fig. 2. The vortex generator, showing vortex ring formation and its use as a short-duration stimulus to fish during natural swimming. (A) Vortex generator set up in the experiment tank with a bluegill sunfish swimming naturally with minimal obstruction. (B) Image of a vortex ring produced using the prototype 1 (of 2) vortex generator during experiments. Food coloring (dye) was used to visualize the vortex ring. (C) Digital particle image velocimetry image of a vortex ring close to impacting the caudal fin of a bluegill sunfish swimming at 0.65 BL s^{-1} . The arrows represent the resultant velocity vectors for the particles constituting the vortex. The maximum velocity is observed in the front and center of the vortex. (D) Illustration of the vortex formation process – when the ball accelerates water out of the cavity, an axial jet is attached to the vortex, called the starting jet. At a certain distance from the ejection point, the vortex separates from the starting jet, and the residual jet is called the trailing jet. L_{stroke} , stroke length; D , cavity diameter; d , orifice diameter. (E) Snapshots from an experimental trial with a live bluegill sunfish swimming at 0.65 BL s^{-1} ($\sim 107 \text{ mm s}^{-1}$). The images show the response of the caudal fin, in the form of deflection from its original position, to a vortex perturbation of known strength. The vortex causes a large deflection in the caudal fin, which is used to estimate the compliance of the fin.

vortices formed quickly and maintained their shape, size and speed for desired travel distances (up to 150 mm) in static and moving water. Vortices interacted with fins for a short duration and caused measurable

deformations in the fins at various tested swimming speeds [$0\text{--}1.5 \text{ body lengths per second (BL s}^{-1})$]. In most experiments, the fish returned to its normal swimming gait after being perturbed.

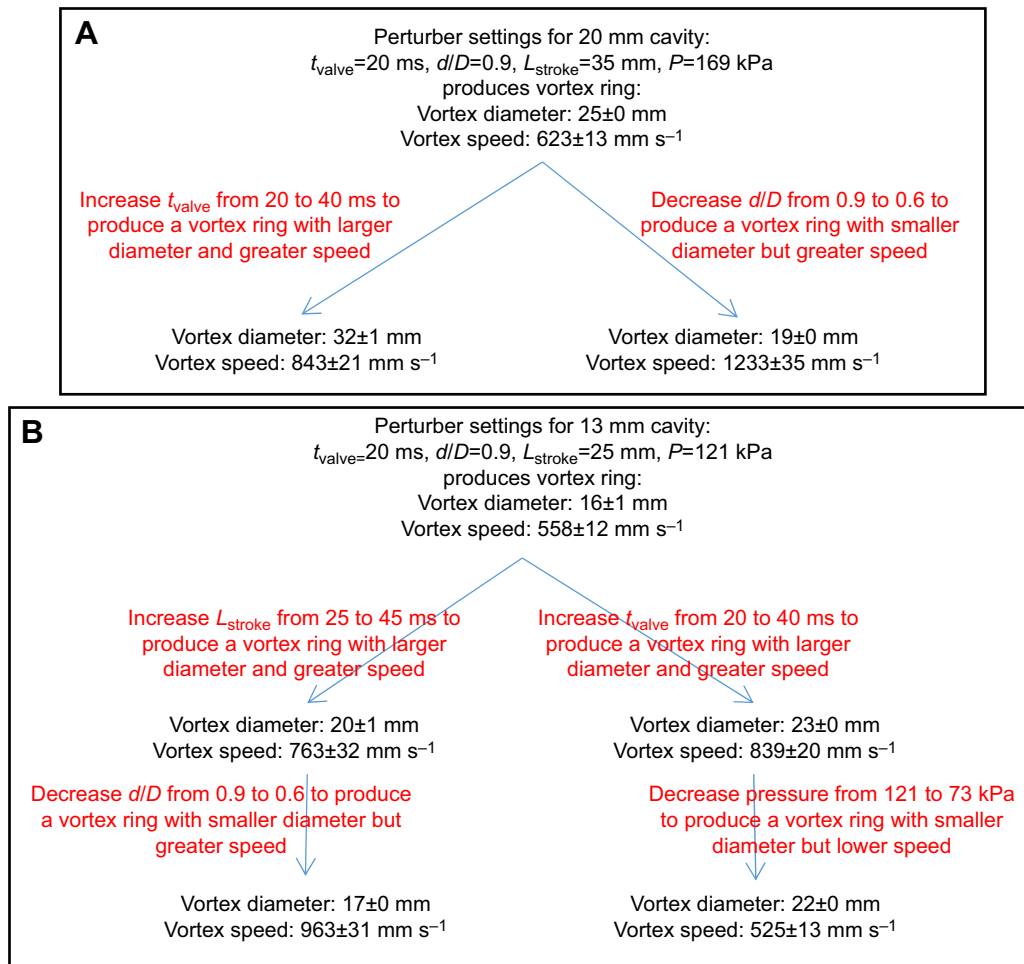


Fig. 3. Examples of how the perturber settings can be altered to tune the size and speed of the resulting vortex to desired settings. The desired perturber settings (pressure, P ; duration for which the valve was open, t_{valve} ; ratio of orifice and cavity diameters, d/D ; and stroke length, L_{stroke}) depended on the testing conditions (the fin that needed to be perturbed, the flow speed, the distance from the perturber at which the fish was swimming, etc.). (A) Examples illustrating a simultaneous change in vortex size and speed by tuning one perturber setting. (B) Examples illustrating a change in only speed (left) or size (right) by tuning two perturber settings. Data are means \pm s.e.m.

Vortex characteristics were well controlled by the perturber settings, which were easily and quickly tuned by the user. Below, we discuss the range of vortex characteristics in static flow and how these characteristics changed with perturber settings.

Separation distance

During formation, the vortices produced by cavity 1 (13 mm) and 2 (20 mm) separated from the starting jet (Fig. 2D) at distances between 0 and 103 ± 1 mm (mean \pm s.e.m.) and between 0 and 113 ± 4 mm, respectively. Separation distance increased with increases in P and t_{valve} , and decreased with increases in d/D . It is important to know this distance so that vortices are not initiated unless fish are positioned beyond the separation distance.

Size of vortex rings

The size of the vortex rings produced using cavity 1 ranged from 14 ± 1 to 27 ± 1 mm (mean \pm s.e.m.) in diameter and 6 ± 0 to 17 ± 2 mm in width, while those produced using cavity 2 ranged from 19 ± 1 to 32 ± 1 mm in diameter and 9 ± 1 to 18 ± 1 mm in width. The size of the vortices increased with increases in P , t_{valve} , d/D and L_{stroke} . Overall, the width increased by a larger percentage than the diameter. For instance, on average, the width increased by 57% while the diameter increased by only 26% when the pressure was increased.

Speed of vortex rings

Vortex rings produced using cavity 1 and 2 traveled at speeds between 371 ± 31 and 2155 ± 31 mm s⁻¹ (mean \pm s.e.m.) and between 464 ± 2 and 1613 ± 25 mm s⁻¹, respectively. The speed of vortices increased with increases in P , t_{valve} and L_{stroke} , and decreased with increases in d/D . Vortex speed was most sensitive to changes in pressure. For example, a 100% increase in pressure caused a 40% increase in speed, but a 100% increase in t_{valve} caused a 3% increase in speed.

Trailing jet

The length of the trailing jet produced during separation ranged from 0 to 100 ± 2 mm and from 0 to 89 ± 1 mm (mean \pm s.e.m.) for cavity 1 and 2, respectively. The length of the trailing jet produced during impact ranged from 0 to 104 ± 3 mm and from 0 to 102 ± 4 mm for cavity 1 and 2, respectively. The trailing jet was measured as 0 mm when there was no visible trailing jet in the videos. For most settings, the length of the trailing jet during impact was smaller for cavity 1 than for cavity 2. The length of the trailing jet increased with increases in P , t_{valve} and L_{stroke} , and decreased with increases in d/D . In some cases, the trailing jet was weak enough to dissipate before vortices made impact. For perturbation studies with fish, the production of a trailing jet was acceptable if the jet did not travel

with the vortex and impact the fish at the same time. Although trailing jets were undesirable, when fast ($>500 \text{ mm s}^{-1}$) vortices were produced, they were unavoidable.

Vortex adjustability

Depending on the desired vortex characteristics, which depended on the experimental conditions such as the fin that needed to be perturbed, flow speed and the fish's position, the perturber settings were altered by the user. As discussed above, a change in a perturber setting (P , t_{valve} , d/D , L_{stroke}) generally caused a change in all the vortex characteristics (size, speed, separation distance, length of trailing jet). To adjust the vortex size and speed simultaneously, one perturber setting could be altered. To adjust only one of the two characteristics, generally two perturber settings needed to be altered. There was more than one way to adjust the vortex characteristics, and Fig. 3 illustrates a few examples of how the vortex size and speed could be adjusted.

Vortices in flow

Vortices maintained their characteristics well under different flow conditions. Flow perpendicular to the direction of vortex travel moved vortices 8 ± 3 to $15 \pm 3 \text{ mm}$ (mean \pm s.e.m.) downstream. An increase in flow speed caused no changes to vortex size, but decreased speed by an average of $16 \pm 1\%$. The increase in speed could be compensated for by changing the perturber settings.

Use of vortices with fish

Vortices caused measurable bending in fins and elicited an active response from multiple fins. Fin bending, measured in the initial 20–40 ms of impact (Fig. 2E), for the caudal fin decreased as the swimming speed increased, suggesting stiffening of the tail at higher speeds. To accurately quantify changes in the fin's stiffness, the force of the vortex can be estimated using circulation and speed measurements (McErlean, 2011), and the deflections caused by a constant force perturbation can be compared at different swimming speeds. The fins also showed an active multi-fin control against disturbances. For example, when the pectoral fin was perturbed at 0.5 BL s^{-1} , it did not show an active change, but the pelvic and caudal fins showed rapid (within 25 ms) changes in area and position. The detailed response of the fish to perturbations and estimates of fin compliance will be discussed in detail in a forthcoming publication.

Conclusions

Perturbation of fins is a key technique that can be used to uncover mechanical properties and control systems that cannot be understood through the study of normal locomotion alone. The generator successfully produced vortex rings of adjustable size and speed that facilitated perturbation experiments with live freely swimming sunfish swimming at different speeds. The circulation of the vortex rings will be measured for all our future biological experiments and will be used to characterize the force of the perturbation. The perturber was designed and built within the size restrictions and allowed an adequate range of motion to either aim at different fins or correct the direction of vortex propagation. The design allowed the control of four design parameters that could be tuned to produce vortex rings with desired characteristics. This device can be used to learn about the mechanical properties of fish

fins as well as to understand how fish use multiple fins to stabilize body position in the face of disturbances.

Acknowledgements

We thank the members of Lauder Lab at Harvard University and Laboratory of Biological Systems Analysis at Drexel University for their help.

Competing interests

The authors declare no competing or financial interests.

Author contributions

Conceptualization, D.S., B.E.F., G.V.L., J.L.T.; Methodology, D.S., B.E.F., G.V.L., J.L.T.; Software, D.S.; Validation, D.S., J.L.T.; Formal Analysis, D.S., J.L.T.; Investigation, D.S., B.E.F., G.V.L., J.L.T.; Resources, D.S., B.E.F., G.V.L., J.L.T.; Data Curation, D.S., J.L.T.; Writing – Original Draft, D.S.; Writing – Review & Editing, G.V.L., B.E.F., J.L.T.; Visualization, D.S.; Supervision, B.E.F., G.V.L., J.L.T.; Project Administration, D.S.; Funding Acquisition, G.V.L., J.L.T.

Funding

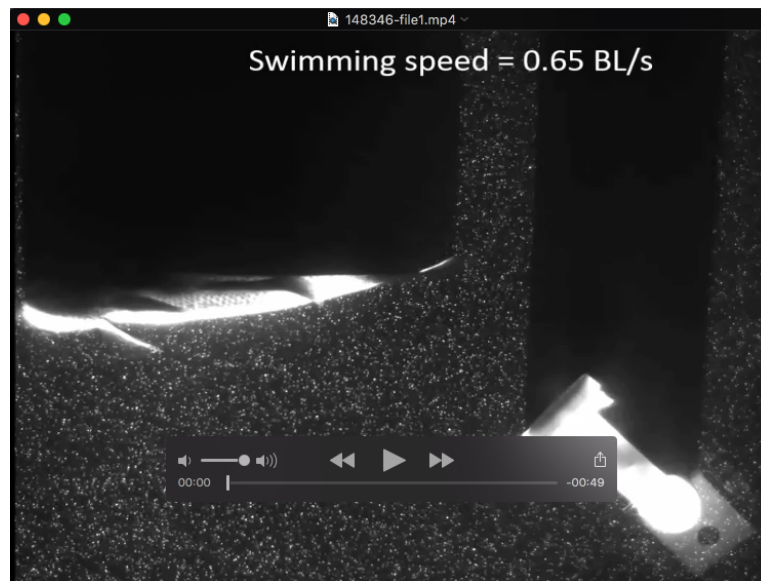
This work was supported by the National Science Foundation (grant NSF CAREER 1150681) and the Office of Naval Research (ONR grant N0001415122234).

Supplementary information

Supplementary information available online at <http://jeb.biologists.org/lookup/doi/10.1242/jeb.148346.supplemental>

References

- Bainbridge, R. (1958). The speed of swimming fish as related to size and to the frequency and amplitude of the tail beat. *J. Exp. Biol.* **35**, 109–133.
- Bennett, D. J., Hollerback, J. M., Xu, Y. and Hunter, I. W. (1992). Time-varying stiffness of human elbow joint during cyclic voluntary movement. *Exp. Brain Res.* **88**, 433–442.
- Curet, O. M., Patankar, N. A., Lauder, G. V. and MacIver, M. A. (2011). Mechanical properties of a bio-inspired robotic knife-fish with an undulatory propulsor. *Bioinspir. Biomim.* **6**, 026004.
- Dabiri, J. O. and Gharib, M. (2005). The role of optimal vortex formation in biological fluid transport. *Proc. R. Soc. B Biol. Sci.* **272**, 1557–1560.
- Flammang, B. E. and Lauder, G. V. (2008). Speed-dependent intrinsic caudal fin muscle recruitment during steady swimming in bluegill sunfish, *Lepomis macrochirus*. *J. Exp. Biol.* **211**, 587–598.
- Flammang, B. E., Alben, S., Madden, P. G. A. and Lauder, G. V. (2013). Functional morphology of the fin rays of teleost fishes. *J. Morphol.* **274**, 1044–1059.
- Gharib, M., Rambod, E. and Shariff, K. (1998). A universal time scale for vortex ring formation. *J. Fluid Mech.* **360**, 121–140.
- Hunter, J. R. and Zweifel, J. R. (1971). Swimming speed, tail beat frequency, tail beat amplitude, and size in jack mackerel, *Trachurus Symmetricus*, and other fishes. *Fish. Bull.* **69**, 253–266.
- Kearney, R. E. and Hunter, I. W. (1982). Dynamics of human ankle stiffness: variation with displacement amplitude. *J. Biomech.* **15**, 752–756.
- Krueger, P. S. and Gharib, M. (2003). The significance of vortex ring formation to the impulse and thrust of a starting jet. *Phys. Fluids* **15**, 1271–1281.
- Long, J. H. and Nipper, K. S. (1996). The importance of body stiffness in undulatory propulsion. *Am. Zool.* **36**, 678–694.
- Long, J. H., Jr, Koob, T. J., Irving, K., Combie, K., Engel, V., Livingston, N., Lammert, A. and Schumacher, J. (2006). Biomimetic evolutionary analysis: testing the adaptive value of vertebrate tail stiffness in autonomous swimming robots. *J. Exp. Biol.* **209**, 4732–4746.
- Marmarelis, P. Z. and Marmarelis, V. Z. (1977). *Analysis of Physiological Systems*. New York: Plenum Press.
- McErlean, M. R. (2011). *Scalability of the Force of a Normally Impacting Vortex Ring on a Planar Surface*. MSc Thesis, Penn State University, State College, PA.
- McHenry, M. J., Pell, C. A. and Long, J. H. (1995). Mechanical control of swimming speed: stiffness and axial wave form in undulating fish models. *J. Exp. Biol.* **198**, 2293–2305.
- Mohseni, K. (2006). Pulsatile vortex generators for low-speed maneuvering of small underwater vehicles. *Ocean Eng.* **33**, 2209–2223.
- Tangorra, J. L., Jones, L. A. and Hunter, I. W. (2003). Dynamics of the human head-neck system in the horizontal plane: Joint properties with respect to a static torque. *Ann. Biomed. Eng.* **31**, 606–620.



Movie S1. Vortex ring perturbation applied to the caudal fin of a Bluegill Sunfish during natural swimming

Vortex ring generated and used as a perturbation to the caudal fin of a Bluegill Sunfish (165 mm total body length) at three different swimming speeds, 0.65, 1.1 and 1.5 body lengths per second, during natural swimming. The video was recorded at 1000 frames per second and is being played at 0.04x speed. Particle image velocimetry was used to visualize the flow during the vortex formation and vortex's interaction with the fish fin.